Published in final edited form as:
Ann Thorac Surg. 2014 October ; 98(4): 1223–1230. doi:10.1016/j.athoracsur.2014.05.026.

Intraoperative Near-Infrared Imaging Can Identify Pulmonary Nodules

Olugbenga T. Okusanya, MD[1], **David Holt**[2], **Daniel Heitjan**[3], **Charuhas Deshpande**[4], **Ollin Venegas**[1], **Jack Jiang**[1], **Ryan Judy**[1], **Elizabeth DeJesus**[1], **Brian Madajewski**[1], **Kenny Oh**, **Steven M. Albelda**[5], **Shuming Nie**[6], and **Sunil Singhal, MD**[1,5,*]

[1]Division of Thoracic Surgery, Department of Surgery, University of Pennsylvania School of Medicine, Philadelphia, Pennsylvania

[2]Department of Clinical Studies, University of Pennsylvania School of Veterinary Medicine

[3]Department of Biostatistics & Epidemiology, University of Pennsylvania

[4]Department of Pathology, University of Pennsylvania School of Medicine

[5]Department of Medicine, University of Pennsylvania School of Medicine

[6]Departments of Biomedical Engineering and Chemistry, Emory University, Atlanta, Georgia

Abstract

Background—Over 80,000 people undergo pulmonary resection for a lung nodule in the United States each year. Small nodules are frequently missed or difficult to find despite preoperative imaging. We hypothesized that near-infrared (NIR) imaging technology could be used to identify and locate lung nodules during surgery.

Methods—We enrolled 18 patients who were diagnosed with a pulmonary nodule that required resection. All patients had a fine-cut 1mm computed tomography scan preoperatively. The patients were given systemic 5 mg/kg indocyanine green (ICG) and then underwent an open thoracotomy 24 hours later. NIR imaging was used to identify the primary nodule and search for additional nodules that were not found by visual inspection or manual palpation of the ipsilateral lung.

Results—Manual palpation and visual inspection identified all 18 primary pulmonary nodules and no additional lesions. Intraoperative NIR imaging detected 16 out of the 18 primary nodules. NIR imaging also identified 5 additional subcentimeter nodules: 3 metastatic adenocarcinomas and 2 metastatic sarcomas. This technology could identify nodules as small as 0.2 cm and as deep as 1.3 cm from the pleural surface. This approach discovered 3 nodules that were in different lobes than the primary tumor. Nodule fluorescence was independent of size, metabolic activity, histology, tumor grade and vascularity.

*Corresponding Author: Sunil Singhal, Division of Thoracic Surgery, University of Pennsylvania School of Medicine, 6 White Building, 3400 Spruce Street, Philadelphia, PA 19104, sunil.singhal@uphs.upenn.edu.

Conclusions—This is the first-in-human demonstration of identifying pulmonary nodules during Thoracic surgery with NIR imaging without *a priori* knowledge of their location or existence. NIR imaging can detect pulmonary nodules during lung resections that are poorly visualized on computed tomography and difficult to discriminate on finger palpation.

Introduction

Approximately 80,000 people undergo thoracic surgery each year to remove a solitary lung nodule(1, 2). Of those patients, 10–15% harbor additional synchronous and metachronous nodules (3–8). At the time of the operation, surgeons typically use visual inspection and finger palpation to search for these lesions. If these nodules are not identified, they can grow over time, require subsequent invasive diagnostic procedures and operations, and cause patient anxiety. With the emergence of minimally invasive pulmonary resections (video assisted thorascopic surgery and robotic surgery), manual palpation is even less common, and the probability of uncovering additional nodules is even decreased (3, 5, 7, 9). Thus, thoracic surgeons need adjuncts to improve their ability to detect pulmonary nodules.

Near-infrared (NIR) image-guided surgery has recently been proposed to identify nodules in solid organs. NIR imaging uses a fluorescent contrast agent and an imaging device to visually enhance abnormal tissue densities. NIR imaging does not use ionizing radiation, can penetrate beyond the organ surface, and provides real time information in the operating room. In the last 10 years, several groups have become interested in using NIR imaging to improve resection of solid organ tumors (10, 11). One study from the Netherlands utilized a non-targeted NIR contrast agent, indocyanine green (ICG), to locate metastatic colorectal tumors in the liver (11). By using the excretory pathways of the biliary system, ICG could provide superior contrast of solid tumors in the liver. A second study from the Netherlands used a targeted fluorophore (fluorescein 520 nm) that bound the folate receptor on ovarian carcinomas (10). In both studies, optical imaging identified additional nodules that were not found on preoperative imaging, visual inspection or manual palpation. To our knowledge, NIR imaging has not been used in thoracic surgery for identifying pulmonary nodules that have not been diagnosed preoperatively.

Based on preclinical data (12, 13) on the enhanced permeability and retention effect (EPR) in lung tissue, we hypothesized that pulmonary nodules could be identified by giving systemic ICG 24 hours prior to surgery. In this study, we enrolled 18 patients undergoing pulmonary resection for excision of a solitary pulmonary nodule. In this pilot study, the chest cavity was imaged to identify all nodules using a NIR camera. We discovered that we could detect a wide histological range of primary nodules independent of nodule size and metabolic activity. Also, we could detect 5 additional nodules that were not identified by any preoperative imaging modality, visual inspection or manual palpation.

Material & Methods

Study Design

This study was approved by the University of Pennsylvania Institutional Review Board and all patients gave informed consent. Any patient with a solitary lung nodule and who was

enrolled for surgery was eligible for this study. All patients underwent computed tomography (CT) scanning with at least 0.1 cm slice thickness. The CT scan was reviewed by a radiologist to confirm the presence of a solitary pulmonary nodule. The patients were specifically consented for the possibility that additional tissue may be resected based on findings from intraoperative NIR imaging, although the magnitude of the operation would not be significantly altered.

During the operation, the surgeons performed a thoracotomy, selectively ventilated the contralateral lung, and located the primary nodule in the deflated lung using visual inspection and manual palpation. The remainder of the ipsilateral lung was inspected independently by both surgeons. Then, the operating room lights were removed, and the NIR imaging system was sterilely draped and positioned above the chest. The primary nodule was imaged and photo-documented by white light and fluorescence. Next, the imaging system was used to search for additional nodules in the ipsilateral lung. Any additional nodules were also resected.

Once removed, all specimens were re-imaged *ex vivo* on a back table in the operating room before submitting to pathology. Frozen section biopsies were performed when indicated. All specimens were sent for permanent histopathology. All nodules were reviewed by a specialized lung pathologist.

NIR Imaging contrast agent

Patients were injected intravenously with 5 mg/kg indocyanine green (ICG) (Akorn Pharmaceuticals, IL) 24 hours prior to surgery. The NIR agent, dose and time point were selected based on extensive preclinical studies from our laboratory (12).

NIR Imaging system

Our intraoperative system was composed of a light source (excitation 740 nm) and two charge-coupled device (CCD) cameras (BioVision, Inc., PA) that were fixed above the operating room table (BioMediCon Inc., NJ). Specific filters split the emitted light from the tissue to a brightfield and a near-infrared camera as previously described (14). The cameras were aligned so an overlay of the two images allowed for precise localization of the fluorescent probes within the tissue. The imaging equipment was mounted inside a 16′×7′×24′ stainless steel case which was stationed above the operating room table. The system was controlled by Metamorph® (Molecular Devices LLC, CA) software that was customized in our laboratory.

Fluorescence Microscopy

5μm thick sections were mounted with a gylcerine-based mounting media. Frozen tumor sections were prepared as previously described (15). The samples were examined using an Olympus® IX51 fluorescent microscope equipped with an indocyanine green specific filter set (Chroma® 49030). Image capture was achieved using a PixeLink® NIR CCD camera (PL-B741EU). Each sample was then subsequently stained with hematoxylin and eosin and re-imaged using white light. Fluorescent images were further processed using ImageJ® (http://rsb.info.nih.gov/ij/; public domain software developed by National Institutes of

Health) to give green pseudo-color to fluorescent signal, and then these images were subsequently overlaid to create color-NIR images.

Immunohistochemistry

Tissues were harvested and bisected with one-half either placed in Tissue-Tek Optimal Cutting Temperature solution and stored at −80°C or in form alin for paraffin sectioning. To detect endothelial cells, monoclonal CD31 (mAB390) was raised from hybridoma supernatant and purified. CD31 expression was quantified by counting the number of positively staining cells in four high-powered (×400) fields.

Data Analysis

We assessed the significance of differences in median values (size, signal-to-background ratio (SBR), depth and Standardized Uptake Value (SUV)) of non-fluorescing vs. fluorescing tumors by the Mann-Whitney test. We assessed correlation of continuous outcomes by the Pearson correlation coefficient. We conducted all analyses in SAS Version 9.3 (SAS Institute, Inc.; Cary, NC). In order to quantitate the amount of fluorescence from the tissue, we used region of interest (ROI) software within ImageJ®. A background reading was taken from adjacent normal lung tissue in order to generate a SBR.

Results

NIR imaging can identify pulmonary nodules intraoperatively

Between January and July 2012, 18 patients between the ages of 29 and 78 (mean 60) with a diagnosis of a solitary pulmonary nodule were evaluated in a Thoracic surgical clinic (Table 1). A 1 mm fine-cut CT scan demonstrated a single pulmonary nodule or mass (0.8–11 cm, mean 2.8 cm). Due to surgeon and/or patient preference, 8 out of 18 patients had a preoperative biopsy by trans-thoracic or trans-bronchial needle aspiration that confirmed a neoplasm. The remaining 10 patients did not have a preoperative tissue diagnosis. All 18 patients were deemed resectable, and they consented to a thoracotomy and pulmonary resection.

During surgery, the operating surgeons palpated the entire lung and reached a consensus that there were no other nodules except for the primary nodule. In order to determine if intraoperative NIR imaging could identify nodules, the entire chest was imaged using the NIR camera (Figures 1 and 2). First, the system was focused on the known primary nodule. Positive NIR imaging defined as an SBR >1.5 and subjective fluorescence identified 14 out of the 18 (78%) primary pulmonary nodules *in situ*. The other 4 primary nodules were not fluorescent through the pleural surface. Next, the remainder of the lung, including the other lobes, was imaged. NIR imaging identified 5 additional nodules that were not detected by CT scan or finger palpation. Of these 5 nodules, two pulmonary nodules were located in the same lobe as the primary nodule. The other 3 nodules were discovered in other lobes in the ipsilateral lung. Finally, all 18 primary pulmonary nodules and 5 secondary pulmonary nodules were then resected either by wedge excision, segmentectomy or anatomic lobectomy. Total NIR imaging time did not exceed 12 minutes in any patient.

In order to determine if the four nodules that did not fluoresce *in situ* were fluorescent at all, the specimen was bi-sected on the back table. Two of the four primary nodules that were not fluorescent were clearly fluorescent once the lung was opened and the nodule was better exposed. The other two primary nodules were not fluorescent even after the lung was opened and the nodule was exposed.

In summary, 21 out of 23 (91%) nodules were fluorescent though only 19 nodules (83%) were fluorescent in the patient (*in situ*). Two nodules were not fluorescent at all (*in situ* or *ex vivo*) (Figure 3).

Subcentimeter pulmonary nodules are fluorescent and visible on NIR imaging

In order to explain why two pulmonary nodules did not fluoresce, we hypothesized that NIR may not be sensitive for small nodules. We found the size and signal-to-background ratio (SBR) of the nodules that could be imaged *in situ* was 0.2–11 cm (mean 2.6) and 1.5–4.4 (mean 2.2), respectively. The size and SBR of the first nodule (patient #4) that did not fluoresce was 1.7 cm and 0.86, respectively. The size and SBR of the second nodule (patient #10) that did not fluoresce was 2.6 cm and 0.85, respectively. Thus, it seemed that nodule fluorescence was independent of size of the nodule. In fact, NIR imaging could identify nodules as small as 0.2 cm.

Nodule fluorescence is independent of histology and metabolic activity

As an alternative explanation for the lack of fluorescence in two nodules, we considered two more variables: histology and metabolic activity.

We examined the histological characteristics such as tumor grade and necrosis may explain the lack of fluorescence in the 2 nodules. Of the 2 nodules that did not fluoresce, one nodule was a contained pulmonary hematoma likely secondary to a chronic pulmonary emboli, and this nodule had a SBR 0.86. The other patient had a single isolated metastatic melanoma to the lung from a back melanoma 12 years earlier, and this nodule did not fluoresce (SBR 0.9).

Of the 21 nodules that did fluoresce, the final pathology demonstrated: 10 adenocarcinomas, 5 squamous cell carcinomas, 3 osteosarcomas, 1 adenosquamous carcinoma, 1 metastatic melanoma and one typical carcinoid tumor (Table 1). Furthermore, we had 1 well-differentiated, 10 moderately differentiated, 6 poorly differentiated nodules, and 6 uncategorized nodules. We found no correlation of any of these variables to SBR. Finally, we also categorized nodules as having no necrosis, minimal necrosis or significant necrosis based on the pathology report. Again, on analysis there were no differences in fluorescence in necrotic nodules.

Nodules that are highly metabolically active are commonly glucose-avid (16). Thus, in order to determine if metabolic activity could predict nodule fluorescence, we correlated the **SUV from the ^{18}** fluorodeoxyglucose positron emission tomography (^{18}FDG-PET) scan to nodule fluorescence. The SUV of the lung nodules ranged from undetected to 56. The two nodules that did not fluoresce had an SUV of 0 and 11. The median SUV did not differ

significantly between the fluorescing and non-fluorescing tumors. The correlation between SUV and SBR was small (r=−0.027) and non-significant (p=0.90).

In situ NIR imaging is limited by the depth of the nodule in the lung

Finally, as an alternative hypothesis to explain why 2 nodules did not fluoresce *in situ*, we postulated that nodules deeper in the lung are difficult to detect due to the limits of NIR imaging technology.

First, we correlated the nodule depth to the nodule fluorescence *in situ*. We assigned the nodule depth as the distance from the pleural surface to the outer rim of the nodule. These measurements were based on the preoperative CT scan, using the closest distance on serial images from coronal, sagittal and axial windows. We found that depth differed significantly by fluorescence (p=0.044), with the non-fluorescing nodules deeper in the lung than the fluorescing nodules (Figure 4a). We found that the nodules that fluoresced were closer to the pleural surface than those that did not (p=0.03). Of the 14 nodules that were detected on preoperative CT scan and fluoresced *in vivo* the mean nodule depth was 0.41 cm (range 0–1.3 cm). Of the 2 nodules that fluoresced *ex vivo* but not *in situ* the mean depth was 1.7 cm.

Then, we postulated that a combination of nodule size and nodule depth may be even a better predictor of detecting a nodule by NIR imaging. We arbitrarily categorized nodules as small (<1.5 cm) or large (>1.5 cm). We found that small nodules fluoresced through the lung surface as long as they were <0.9 cm from the surface. Indeed, larger nodules fluoresced through the lung surface as far as 1.3 cm from the pleural surface. Subjectively, we noted that nodules that puckered the pleural surface were more fluorescent than nodules that did not affect the surface of the lung.

In summary, nodule depth is important in predicting *in situ* fluorescence, and this is independent of nodule size. Subcentimeter nodules have approximately 1 cm depth of penetration though larger nodules can be imaged slightly deeper in the lung.

The degree of nodule fluorescence is independent of size and vascularity

For the nodules that fluoresced, we hypothesized that the *amount* of nodule fluorescence (ie. signal-to-background ratio) may be dependent on the size of the nodule or the degree of vascularity (12).

We correlated the measurement of each resected nodule to its SBR. We found the size of the 21 fluorescent pulmonary nodules (16 primary nodules, 5 secondary nodules) ranged from 0.2 to 11 cm (mean 2.5). The SBR of these nodules varied from 0.85 to 4.4 (mean 1.9). The Pearson correlation of size and SBR was r=0.63 (p=0.002). Thus, there was not a strong correlation between size and the degree of fluorescence. However, we then categorized the nodules as less than 2 cm and greater than 3 cm to examine opposite ends of the spectrum. In this situation, we found a tendency for smaller nodules to be less fluorescent, however, this did not reach statistical significance (Figure 4b).

Finally, we examined nodule vascularity in relation to fluorescence. We and others have previously published from rodent models that highly vascular nodules are more likely to

fluoresce due to improved diffusion of the fluorophore into the nodule (12). Nodule vascularity was quantified by CD31 immunostaining as 0^+ (avascular), 1^+ (poorly vascular), 2^+ (moderately vascular) and 3^+ (highly vascular). Surprisingly, there was no association of nodule vascularity with nodule fluorescence (Figure 4c). The chronic pulmonary embolus in patient #4 was completely avascular and did not fluoresce, however the metastatic melanoma in patient #10 was not avascular (2^+ CD31 staining) yet it did not fluoresce.

Comment

The goal of this study was to determine if NIR imaging could identify pulmonary nodules during a lung resection. In this pilot study, 18 patients with a solitary pulmonary nodule underwent a thoracotomy after systemic injection of 5 mg/kg ICG. NIR signal detected 91% of these primary nodules suggesting co-localization of the ICG to the nodules, and fluorescent microscopy confirmed the ICG was in the tumors. NIR imaging interestingly also detected 5 additional nodules. The sensitivity for detecting fluorescent pulmonary nodules was dependent on the depth of the nodule in the lung but independent of nodule size, metabolic activity, histology and vascularity.

An important discovery from this study is that NIR imaging can detect subcentimeter pulmonary nodules that are difficult to detect by conventional techniques. CT scanning has a limited sensitivity for nodules less than 1 cm, even with 0.1 cm slice thickness images. Many nodules in the 0.1–0.4 cm range are ignored as artifact or are too small to address. Finger palpation is also used to survey the lung for pulmonary nodules. However, this is highly dependent on the experience and judgment of the surgeon and has a high degree of human error. We showed that NIR imaging can readily detect abnormalities as small as 0.2 cm.

Other techniques for intraoperative detection of pulmonary nodules such as pulmonary ultrasound, radionucleotide imaging, CT-guided and spiral wire localization require *a priori* information on the location of nodule and can be technically challenging (17–20). NIR imaging has several unique advantages compared to other techniques. First, it does not require radiation. The excitation energy for exciting NIR contrast agents is low (10^{-1} eV) and has less energy than the lights in an operating room, thus it is safe for humans without shielding. Second, optical visible (390–750 nm) probes (i.e. fluorescein, methylene blue) have no penetration due to tissue scattering and blood absorption, thus NIR dyes (750–900 nm) are better imaged through organs. Third, NIR imaging does not require advance knowledge of the location of the nodule and can image large surfaces simultaneously. Lastly, NIR imaging is easy to understand, real-time and intuitive for the observer.

NIR imaging depends on a scanning device and an intravenous contrast agent (21). There are currently several available NIR imaging cameras for intraoperative use including the Artemis (Quest Medical Imaging, Inc.), Pinpoint (Novadaq, Inc.), the Karl Storz PPD unit and the Firefly System (Intuitive, Inc.). For this study, we developed an inexpensive custom-made imaging unit (Biovision©, PA) that has been previously described (14). (14)Importantly, these systems now have minimally invasive and robotic capabilities. Currently, there is only one NIR fluorophore, ICG, that is FDA approved for clinical use in

humans in the United States. ICG is a water-soluble anionic, amphiphilic fluorophore that is particular attractive due to its excitation (λ_{ex} 778 nm) and emission (λ_{em} 830 nm). When given systemically, it binds rapidly to plasma proteins and lipoproteins in the vascular compartment (22). ICG has been strongly hypothesized to be retained in nodules, tumors and areas of inflammation by the non-receptor specific enhanced permeability and retention effect (EPR) (12). The EPR effect, first described in 1986 by Matsumura and Maeda, is a property by which small molecules such as ICG passively accumulate in tumors due to the presence of defective endothelial cells and wide fenestrations (600 to 800 nm) in nascent blood vessels (23). Once in the tumor microenvironment, these particles are retained due to global properties such as molecular size, shape, charge and polarity, rather than tumor-specific targeting mechanisms such as ligand-receptor interactions (24).

This pilot study demonstrated two limitations to NIR imaging for pulmonary nodules. First, the depth of penetration is an important drawback. The maximum depth of penetration for imaging a nodule was 1.3 cm. This depth of penetration is somewhat arbitrary because our calculations were based on measurements from an inflated lung on a CT scan. In actuality, in the deflated, atelectatic lung, the depth of penetration is likely to be different. Thus, its application to other solid organs will need to be independently assessed. The second limitation is the failure to identify 2 nodules. Despite the best of our attempts to explain this finding, the reasons remain unclear. We demonstrated that the pulmonary embolus was avascular and lacked epithelial cells, thus suggesting one possible explanation. However, the metastatic melanoma was vascular, though it also lacked epithelial cells. Although NIR dyes supposedly diffuse into abnormal and inflamed tissues due to hyperpermeable vascular structures, we believe that there is some active binding of NIR dyes to epithelial cells or the binding is related to differences in cancer cell surface electromagnetic potentials. Further studies will need to be conducted as we encounter more nodules that do not fluoresce.

We acknowledge several caveats to this study. First, this is a pilot study; therefore the study size is small. In addition, as mentioned above, the lung deflates during thoracotomy, thus we cannot precisely determine the true depth of penetration of NIR imaging. Finally, SUV is an arbitrary number and not a true measure of tissue metabolism. Thus, correlating metabolism to fluorescence may not accurately represent the biology of the nodule.

There are several potential directions to expand our imaging strategy. First, new emerging imaging technologies will allow better depth of penetration into the lung. Work in diffuse optical tomography and alternative imaging devices that capture scattering can measure fluorescence deeper in organs. Second, novel contrast agents such as targeted NIR dyes that provide information about nodule phenotype are being developed for clinical use (10, 25). For example, folate receptor alpha (FRα) is expressed in 70–90% of lung adenocarcinomas. Thus, several groups are developing optical contrast agents to selectively target FRα+ lung tumors (clinicaltrials.gov: NCT01335893). Third, we realize that there are other variables that could be altered to improve tissue fluorescence such as the amount of contrast dye administered and the interval from injection to imaging. Fourth, it will be interesting to apply this technology to the detection of nodules in other solid organs such as the breast, kidney, colon, pancreas and prostate. The lung has no auto-fluorescence in the NIR range, thus it is an excellent application of this technology. Our next study will be to apply this

technology in a minimally invasive setting and specifically for the identification of subcentimeter pulmonary nodules that are difficult to locate without tactile information.

Acknowledgments

This work was supported by the National Institutes of Health R01 CA163256 (DH, MW, SN, SS), Society of Surgical Oncology (SS) and the CHEST Foundation (SS). The authors would like to acknowledge Andrew Tsourkas, PhD for his scientific input.

References

1. 2013 united states procedure volumes database. Thomas reuters; United States: 2013.
2. National inpatient sample (nis). Agency for healthcare research and quality. 2011. Http://www.Hcup-us.Ahrq.Gov/nisoverview.Jsp
3. Cerfolio RJ, Bryant AS. Is palpation of the nonresected pulmonary lobe(s) required for patients with non-small cell lung cancer? A prospective study. J Thorac Cardiovasc Surg. 2008; 135(2):261–268. [PubMed: 18242247]
4. Cerfolio RJ, Bryant AS, McCarty TP, Minnich DJ. A prospective study to determine the incidence of non-imaged malignant pulmonary nodules in patients who undergo metastasectomy by thoracotomy with lung palpation. Ann Thorac Surg. 2011; 91(6):1696–1700. discussion 1700-1691. [PubMed: 21619965]
5. Cerfolio RJ, McCarty T, Bryant AS. Non-imaged pulmonary nodules discovered during thoracotomy for metastasectomy by lung palpation. Eur J Cardiothorac Surg. 2009; 35(5):786–791. discussion 791. [PubMed: 19237294]
6. Diederich S, Das M. Solitary pulmonary nodule: Detection and management. Cancer Imaging. 2006; 6:S42–46. [PubMed: 17114077]
7. Ellis MC, Hessman CJ, Weerasinghe R, Schipper PH, Vetto JT. Comparison of pulmonary nodule detection rates between preoperative ct imaging and intraoperative lung palpation. Am J Surg. 2011; 201(5):619–622. [PubMed: 21545910]
8. Mineo TC, Ambrogi V, Paci M, Iavicoli N, Pompeo E, Nofroni I. Transxiphoid bilateral palpation in video-assisted thoracoscopic lung metastasectomy. Arch Surg. 2001; 136(7):783–788. [PubMed: 11448391]
9. McCormack PM, Bains MS, Begg CB, et al. Role of video-assisted thoracic surgery in the treatment of pulmonary metastases: Results of a prospective trial. Ann Thorac Surg. 1996; 62(1):213–216. discussion 216–217. [PubMed: 8678645]
10. van Dam GM, Themelis G, Crane LM, et al. Intraoperative tumor-specific fluorescence imaging in ovarian cancer by folate receptor-alpha targeting: First in-human results. Nat Med. 2011
11. van der Vorst JR, Schaafsma BE, Hutteman M, et al. Near-infrared fluorescence-guided resection of colorectal liver metastases. Cancer. 2013; 119(18):3411–3418. [PubMed: 23794086]
12. Madajewski B, Judy BF, Mouchli A, et al. Intraoperative near-infrared imaging of surgical wounds after tumor resections can detect residual disease. Clin Cancer Res. 2012; 18(20):5741–5751. [PubMed: 22932668]
13. Singhal S, Nie S, Wang MD. Nanotechnology applications in surgical oncology. Annu Rev Med. 2010; 61:359–373. [PubMed: 20059343]
14. Okusanya OT, Madajewski B, Segal E, et al. Small portable interchangeable imager of fluorescence for fluorescence guided surgery and research. Technol Cancer Res Treat. 2013
15. Predina J, Eruslanov E, Judy B, et al. Changes in the local tumor microenvironment in recurrent cancers may explain the failure of vaccines after surgery. Proc Natl Acad Sci U S A. 2013; 110(5):E415–424. [PubMed: 23271806]
16. Jacobson O, Chen X. Interrogating tumor metabolism and tumor microenvironments using molecular positron emission tomography imaging. Theranostic approaches to improve therapeutics. Pharmacol Rev. 2013; 65(4):1214–1256. [PubMed: 24064460]

17. Eichfeld U, Dietrich A, Ott R, Kloeppel R. Video-assisted thoracoscopic surgery for pulmonary nodules after computed tomography-guided marking with a spiral wire. Ann Thorac Surg. 2005; 79(1):313–316. discussion 316–317. [PubMed: 15620965]

18. Powell TI, Jangra D, Clifton JC, et al. Peripheral lung nodules: Fluoroscopically guided video-assisted thoracoscopic resection after computed tomography-guided localization using platinum microcoils. Ann Surg. 2004; 240(3):481–488. discussion 488–489. [PubMed: 15319719]

19. Chella A, Lucchi M, Ambrogi MC, et al. A pilot study of the role of tc-99 radionuclide in localization of pulmonary nodular lesions for thoracoscopic resection. Eur J Cardiothorac Surg. 2000; 18(1):17–21. [PubMed: 10869935]

20. Zaman M, Bilal H, Woo CY, Tang A. In patients undergoing video-assisted thoracoscopic surgery excision, what is the best way to locate a subcentimetre solitary pulmonary nodule in order to achieve successful excision? Interact Cardiovasc Thorac Surg. 2012; 15(2):266–272. [PubMed: 22572410]

21. Sevick-Muraca EM. Translation of near-infrared fluorescence imaging technologies: Emerging clinical applications. Annu Rev Med. 2012; 63:217–231. [PubMed: 22034868]

22. Yoneya S, Saito T, Komatsu Y, Koyama I, Takahashi K, Duvoll-Young J. Binding properties of indocyanine green in human blood. Invest Ophthalmol Vis Sci. 1998; 39(7):1286–1290. [PubMed: 9620093]

23. Matsumura Y, Maeda H. A new concept for macromolecular therapeutics in cancer chemotherapy: Mechanism of tumoritropic accumulation of proteins and the antitumor agent smancs. Cancer Res. 1986; 46(12 Pt 1):6387–6392. [PubMed: 2946403]

24. Heneweer C, Holland JP, Divilov V, Carlin S, Lewis JS. Magnitude of enhanced permeability and retention effect in tumors with different phenotypes: 89zr-albumin as a model system. J Nucl Med. 2011; 52(4):625–633. [PubMed: 21421727]

25. van de Ven SM, Elias SG, Chan CT, et al. Optical imaging with her2-targeted affibody molecules can monitor hsp90 treatment response in a breast cancer xenograft mouse model. Clin Cancer Res. 2012; 18(4):1073–1081. [PubMed: 22235098]

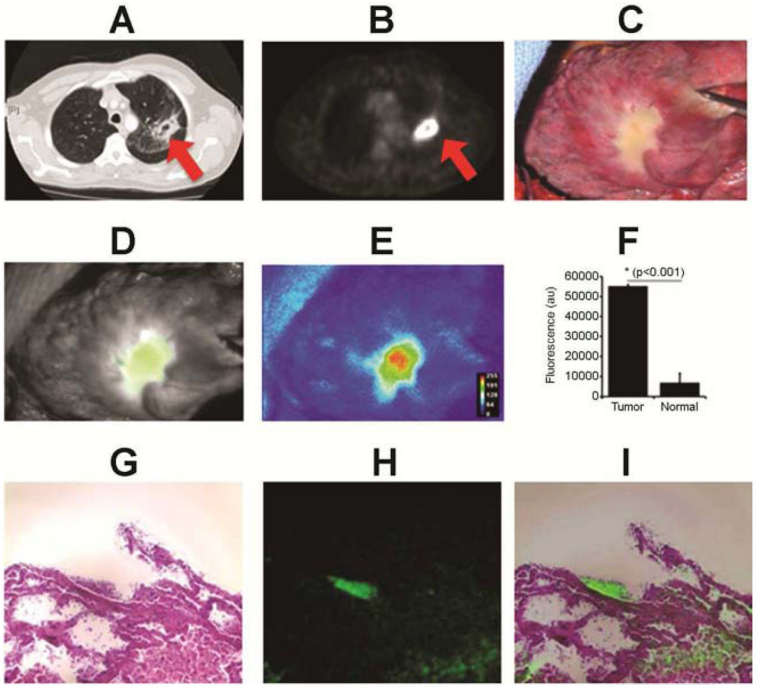

Figure 1.

Patient #3: A 64 year old female presented with a ^{18}FDG-avid (SUV 9.3) 6 cm right upper lobe tumor. (A) CT scan; (B) PET scan; (C) Conventional camera; (D) Near-infrared camera; (E) Near-infrared heat map; (F) Fluorescence; (G) Hematoxylin & Eosin; (H) 780 nm light source; (I) Miscroscopic overlay.

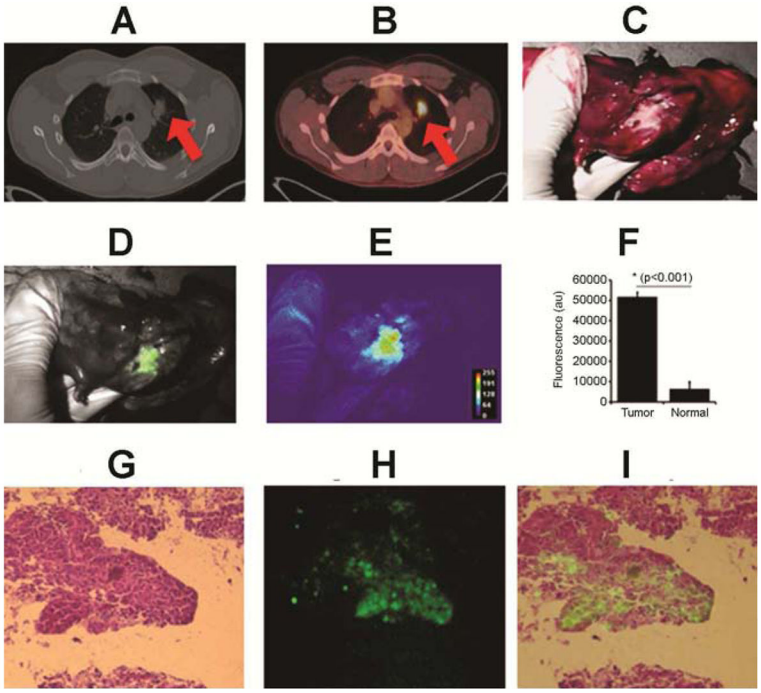

Figure 2.

Patient #12: A 29 year old male presented with a ^{18}FDG-avid (SUV 7) 2.7 cm right upper lobe tumor.

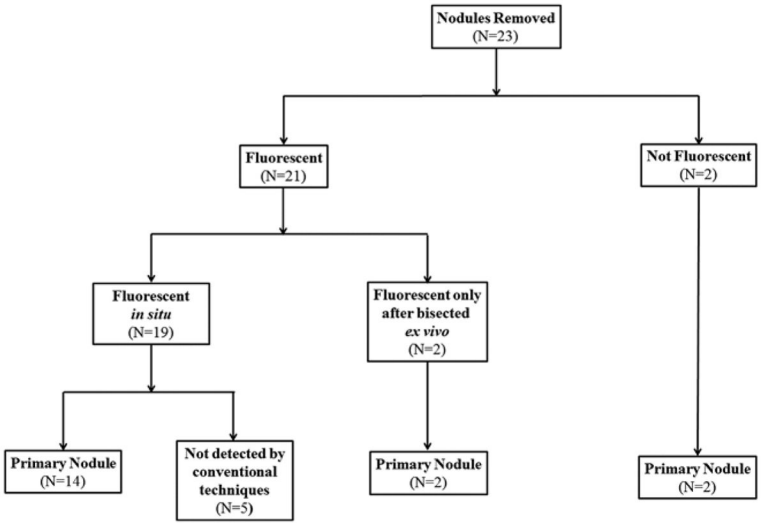

Figure 3.
Overview of results from NIR imaging study.

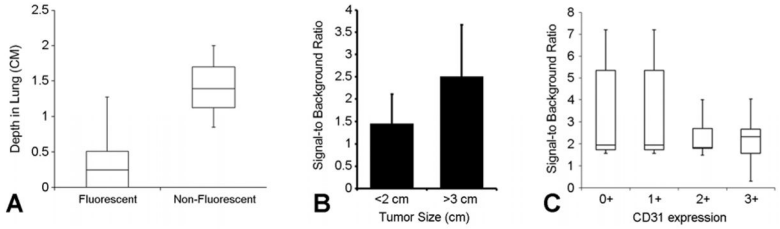

Figure 4.

A. *In situ*, fluorescent nodules are more likely to be closer to the pleural surface (p=0.044).

B. Smaller nodules (<2 cm) trended towards less fluorescence but this did not reach statistical significance nor did it have clinical impact.

C. There is no correlation of microvascular density (CD31 staining) to degree of fluorescence.

Table 1

Characteristics of pulmonary nodules removed from 18 patients who underwent pulmonary resection.

	Not Fluorescent	Fluorescent
N	2	21
Signal-to-background ratio (SBR)	0.85	1.5 – 4.4 (mean 2.2)
Size (cm)	1.9, 2.3	0.2 – 11 (mean 2.6)
Depth from surface (cm)	0, 0.6	0 – 1.3 (mean 0.4)
Standardized uptake value (SUV)	0, 11	Undetected – 56 (median 9.1)
Pathology	Chronic pulmonary emboli (1) Melanoma (1)	Adenocarcinoma 910) Squamous cell carcinoma (5) Osteosarcoma (3) Melanoma (1) Adenosquamous (1) Typical carcinoid (1)